Total reaction and partial cross section calculations in proton-nucleus ($Z_t \leq 26$) and nucleus-nucleus reactions (Z_p and $Z_t \leq 26$)

L. Sihver,[1] C. H. Tsao,[2] R. Silberberg,[3] T. Kanai,[1] and A. F. Barghouty[4]
[1]*National Institute of Radiological Sciences (NIRS), Chiba-shi, Inage-ku, Anagawa 4-9-1, Chiba 263, Japan*
[2]*Naval Research Laboratory, Washington, D.C. 20375*
[3]*University Space Research Association, Washington, D.C. 20024*
[4]*Physics Department, Roanoke College, Salem, Virginia 24153*
(Received 2 October 1992)

We have developed semiempirical total reaction cross section formulas for proton-nucleus (with $Z_t \leq 26$) and nucleus-nucleus (with Z_p and $Z_t \leq 26$) reactions. These formulas apply for incident energies above ≈ 15 MeV and ≈ 100 MeV/nucleon, respectively. We have also constructed a procedure for calculating the projectile-fragment production cross sections, by scaling semiempirical proton-nucleus partial cross section systematics. The scaling is done by a scaling parameter, which is based on a Bradt-Peters-type law and also takes advantage of the weak-factorization property of projectile fragments. All products from the Z of the projectile down to $Z=2$ can be calculated. The agreement between the calculated partial cross sections and the experimental data is better than all earlier published results.

PACS number(s): 25.70.Mn

I. INTRODUCTION

The interaction and propagation of high-energy heavy ions in matter is a subject of much current interest and activity. One fundamental observable is the total reaction cross section, which is defined as the total minus the elastic cross sections for nucleons incident on a nucleus:

$$\sigma_R = \sigma_T - \sigma_{\rm el} \ . \tag{1}$$

To understand the nuclear strong interactions, the basic properties of the reaction cross sections are needed. To know the reaction cross sections is also very important in many other research areas, including shielding against heavy ions originating from either space radiations or accelerators, cosmic ray propagation, radiobiological effects resulting from work, or clinical exposures [1]. The total reaction cross section has therefore been extensively studied both theoretically and experimentally for more than 45 years. A detailed list of references is found in Ref. [2], by Kox *et al.*

We have chosen to describe the total reaction cross sections by semiempirical equations, and we have developed new parameters for these formulas. Our parameters apply for incident energies above ≈ 15 MeV and ≈ 100 MeV/nucleon for proton-nucleus (with $Z_t \leq 26$) and nucleus-nucleus (with Z_p and $Z_t \leq 26$) reactions, respectively.

When a heavy-ion beam impinges upon a target, the collision can result in nuclear fragmentation. Depending on impact parameters, these events are characterized as projectile and/or target fragmentation. On the one hand, the target fragments are typically large, high Z fragments, which carry little momentum. On the other hand, the projectile fragments lose very little momentum and travel nearly in the beam direction with relatively minor deflection.

The partial nucleus-nucleus cross sections of high-energy reactions are of considerable astrophysical interest. They are also of great importance in therapeutic and diagnostic medicine [1], since the projectile fragments lower the average stopping power relative to that of the incident beam. They will therefore make up a "tail," which extends beyond the stopping region of the primary beam (i.e., beyond the Bragg peak).

Silberberg and Tsao [3] have developed a semiempirical systematics for calculation of these cross sections for proton-nucleus reactions. They have also developed equations for calculating the cross sections for the break-up of nuclides (Z_i, A_i) colliding with (Z_j, A_j) by scaling their semiempirical systematics [4–6]. However, these equations are based on a first iteration and the agreement with experimental data needs improvement. Cummings *et al.* [7] have developed a procedure to calculate the fragmentation cross sections for both hydrogen targets and "heavy" targets, by fitting experimental data. However, there has not been any attempt to make these fits for "light" ($Z \leq 26$) projectile-target combinations yet. We have therefore constructed a procedure for calculating these cross sections, by scaling semiempirical proton-nucleus partial cross section systematics. All products from the Z of the projectile down to $Z=2$ can be calculated. The scaling is done by a scaling parameter, which is based on a Bradt-Peters-type law and also takes advantage of the weak-factorization property of projectile fragments. Additional enhancement factors for single-nucleon stripping, large ΔA reactions, and the lightest products (Li, Be, and B) are also added. The agreement between the calculated cross sections and the experimental data is better than all earlier published results.

II. TOTAL REACTION CROSS SECTIONS

From geometrical arguments, one expects the total reaction cross section σ_R for proton-nucleus reactions to be

proportional to the area "seen" by the projectile, i.e., to πR^2, R being the nucleus radius. Since $R \propto A^{1/3}$, one expects a dependence of the form $\sigma_R \propto A^{2/3}$. For nucleus-nucleus reactions, one expects a dependence of the form $\sigma_R \propto (A_p^{1/3}+A_t^{1/3})^2$. The first empirical expression of the total reaction cross section σ_R for nucleus-nucleus collisions was proposed by Bradt and Peters [8],

$$\sigma_{\text{reac}}=\pi r_0^2(A_p^{1/3}+A_t^{1/3}-b_0)^2 , \tag{2}$$

where A_p and A_t are the mass numbers of the projectile and the target, respectively, and b_0 is the overlap or transparency parameter, and r_0 is the constant of proportionality in the expression for the geometrical nuclear radius $r_i=r_0 A_i^{1/3}$. Both b_0 and r_0 are energy-independent parameters. Although adequate for high energies ≥ 1.5 GeV/nucleon, where both the total cross sections and the total reaction cross sections are expected to be energy independent, there are significant differences between the calculated values and the experimental data at energies below 1.5 GeV/nucleon. Therefore there have been many modifications of this formula, with both energy-independent [9–14] and energy-dependent parameters [15]. Others [16] have tried to develop expressions which depend on the sum of the target and projectile mass, as can be expected for peripheral reactions.

A. Proton-nucleus reactions

1. *High-energy formula*

We have studied the following energy-independent formula, originally developed for nucleus-nucleus interactions [12,13]:

$$\sigma_{\text{reac}}=\pi r_0^2[A_p^{1/3}+A_t^{1/3}-b_0(A_p^{-1/3}+A_t^{-1/3})]^2 , \tag{3}$$

where $r_0=1.36$ fm.

The proton-nucleus reaction cross sections drops above 30 MeV until about 100–200 MeV, where it settles at a value which remains approximately unchanged up to around 500 MeV [17]. The energy dependence for incident energies above 200 MeV is roughly of the same order as the experimental errors. Therefore we assume energy independence for incident energies above 200 MeV. To adapt it to proton-nucleus reactions, we first set $A_p=1$ and then express b_0 as a polynomial function of the first order in $(1+A_t^{-1/3})$. Our high-energy formula is then

$$\sigma(p,N)_{\text{reac}}=\pi r_0^2[1+A_t^{1/3}-b_0(1+A_t^{-1/3})]^2 , \tag{4}$$

$$b_0=2.247-0.915(1+A_t^{-1/3}) , \tag{5}$$

for $E_p \geq 200$ MeV and $r_0=1.36$ fm.

2. *Energy dependence at low energies*

For incident energies below 200 MeV, we cannot assume energy independence. To calculate the energy dependence at these energies, we have developed energy-dependent functions. These functions are then multiplied by our energy-independent function. Equations (6)–(8) are our energy-dependent total reaction cross section formulas:

$$\sigma(E,p,N)_{\text{reac}}=0.14e^{0.0985E}f(E,p,N)_{\text{reac},1}\sigma(p,N)_{\text{reac}} , \tag{6}$$

for $E_p<20$ MeV and $6\leq Z_t\leq 8$, or

$$\sigma(E,p,N)_{\text{reac}}=f(E,p,N)_{\text{reac},1}\sigma(p,N)_{\text{reac}} , \tag{7}$$

for $20\leq E_p\leq 150$ MeV and $6\leq Z_t\leq 8$ and for $Z_t<6$ or $Z_t>8$ and $E_p\leq 150$ MeV,

$$\sigma(E,p,N)_{\text{reac}}=f(E,p,N)_{\text{reac},1}f(E,p,N)_{\text{reac},2}\sigma(p,N)_{\text{reac}} + f(E,p,N)_{\text{reac},3}f(p,N)_{\text{reac}} , \tag{8}$$

for $150\leq E_p<200$ MeV. The energy-dependent functions are written as

$$f(E,p,N)_{\text{reac},1}=1.15+\lambda_1 e^{-E/\lambda_2}(1-0.62e^{-E/200}) \times\sin(10.9E^{-0.28}) ,$$

$$f(E,p,N)_{\text{reac},2}=4.00-0.02E ,$$

$$f(E,p,N)_{\text{reac},3}=0.02E-3.00 .$$

λ_1 is 1.4 if $Z_p\leq 8$ and 0 otherwise. λ_2 is 38 if $Z_p=4$, 25 if $Z_p=5$, 10 if $6\leq Z_p\leq 8$, and 1 otherwise. E is the incident kinetic proton energy.

No attempt to model the resonance features at low energies has been made. The above formulas can also be used to calculate the total reaction cross sections for reactions between heavy ions and hydrogen. In Fig. 1 we show examples of the calculated cross sections, together with the experimental data [17], for the reactions of protons with Be, B, C, and Al, respectively. In Table I all the cross sections shown in Fig. 1 are tabulated. In Fig. 2 we show $\sigma(\text{calc})/\sigma(\text{expt})$ for the reactions of protons with different targets, ranging from Be to Fe.

B. Nucleus-nucleus reactions

To calculate the nucleus-nucleus reaction cross sections, we also use Eq. (2) and assume energy independence for incident energies ≥ 100 MeV/nucleon. The overlap parameter b_0 is expressed as a polynomial function of the first order in $(A_p^{-1/3}+A_t^{-1/3})$, similar to the proton-nucleus reactions:

$$\sigma(N,N)_{\text{reac}}=\pi r_0^2[A_p^{1/3}+A_t^{1/3}-b_0[A_p^{-1/3}+A_t^{-1/3}]^2 , \tag{9}$$

$$b_0=1.581-0.876(A_p^{-1/3}+A_t^{-1/3}) . \tag{10}$$

In Fig. 3 we show the ratio $\sigma_{\text{calc}}/\sigma_{\text{expt}}$ as a function of $(A_p^{1/3}+A_t^{1/3})$. From this figure we can see that Eq. (2), with $b_0=1.581-0.876(A_p^{-1/3}+A_t^{-1/3})$, gives a good agreement with the experimental data for most of the collision systems studied.

The first 400-MeV/nucleon ^{20}Ne beam was delivered by SIS, GSI, recently, and the first measurements of the fragmentation of this beam in water was done [18]. A

stack of four 500-μm-thick silicon detectors was used, and the attenuation of the primary ^{20}Ne ions was obtained by gating on the $Z=10$ peak distribution. The measured mean free path was 163±8 mm. We have calculated this mean free path, using our reaction cross section formulas. Our calculated value is 163 mm, i.e., in total agreement with the experimental value.

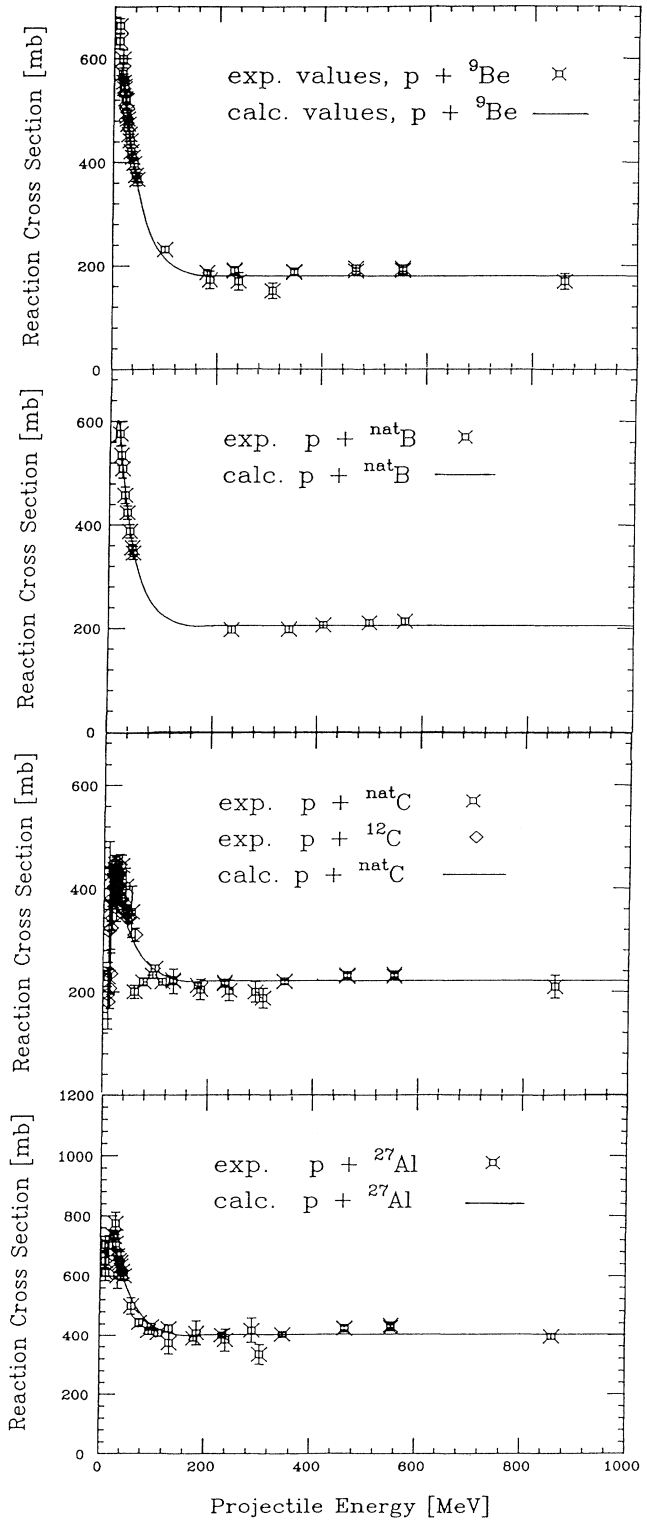

FIG. 1. Calculated σ_R, together with experimental data [17], for the reactions of protons with Be, B, C, and Al.

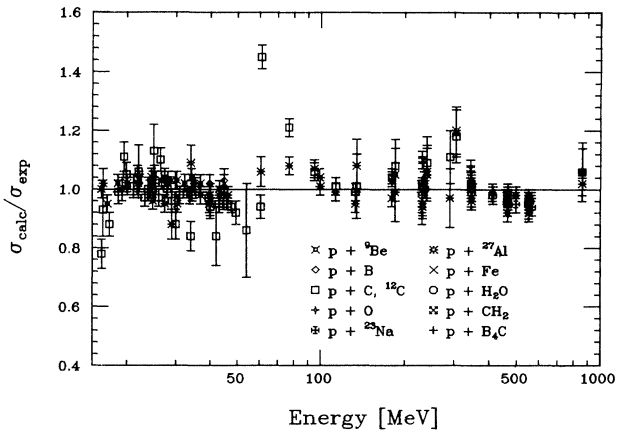

FIG. 2. Ratios σ(calc)/σ(reac) as function of incident energy for the reactions of protons with different targets ranging from Be to Fe. The experimental data are taken from Ref. [17].

III. NUCLEUS-NUCLEUS PARTIAL CROSS SECTIONS

The partial inelastic cross sections have systematic regularities that permit the formulation of semiempirical equations. Rudstam [19–21] noted these systematic regularities and developed a semiempirical cross section formula which is particularly useful for targets heavier than calcium. This should not be applied to light product nuclei, particularly at low energies. Rudstam's equation is

$$\sigma=\sigma_0 e^{-P\Delta A}e^{-R|Z-SA+TA^2|^{3/2}} . \tag{11}$$

The factor $(-p\Delta A)$ describes the diminution of cross sections as the difference of target and product mass, ΔA, increases. The factor $\exp(-R|Z-SA+TA^2|^{\nu})$, with $\nu\approx\frac{3}{2}$, describes the distribution of cross sections for the

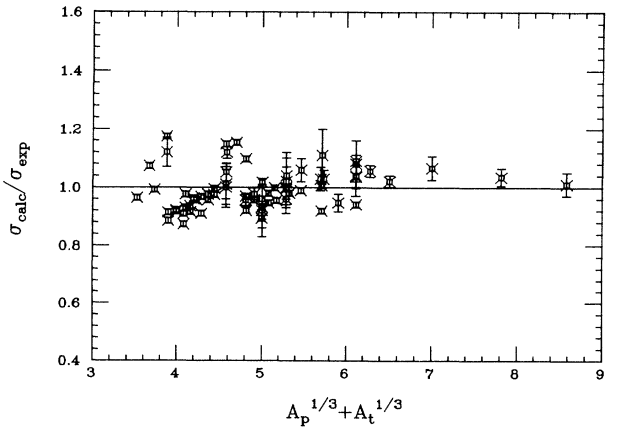

FIG. 3. σ(calc)/σ(reac) as function of $(A_p^{1/3}+A_t^{1/3})$ for nucleus-nucleus reactions above 100 MeV/nucleon. The experimental data are taken from Refs. [2, 29–35].

TABLE I. Proton-nucleus reaction cross sections.

Nucleus	Energy (MeV)	Calculated σ_R (mb)	Experimental σ_R (mb)	$\frac{\sigma(\text{calc})}{\sigma(\text{expt.})}$
^{9}Be	16.2	575	571±18	1.01±0.03
^{9}Be	17.0	572	599±17	0.95±0.03
^{9}Be	18.5	555	565±15	0.98±0.03
^{9}Be	20.0	555	542±15	1.02±0.03
^{9}Be	20.1	554	547±19	1.01±0.03
^{9}Be	21.9	540	530±16	1.02±0.03
^{9}Be	22.1	539	523±18	1.03±0.03
^{9}Be	24.2	521	519±17	1.00±0.03
^{9}Be	24.5	518	497±14	1.04±0.03
^{9}Be	25.1	513	489±16	1.05±0.03
^{9}Be	26.6	500	484±17	1.03±0.03
^{9}Be	27.3	494	474±14	1.04±0.03
^{9}Be	28.0	488	474±13	1.03±0.03
^{9}Be	30.2	469	454±13	1.03±0.03
^{9}Be	32.2	453	442±13	1.02±0.03
^{9}Be	34.2	437	421±13	1.04±0.03
^{9}Be	36.8	417	410±12	1.02±0.03
^{9}Be	39.7	379	398±12	0.95±0.03
^{9}Be	43.1	376	375±12	1.00±0.03
^{9}Be	46.2	358	367±12	0.98±0.03
^{9}Be	99.3	214	231±6	1.04±0.03
^{9}Be	180.0	180	186±5	0.97±0.03
^{9}Be	185.0	180	172±17	1.05±0.09
^{9}Be	232.0	180	189±7	0.95±0.04
^{9}Be	232.0	180	191±7	0.94±0.04
^{9}Be	240.0	180	169±17	1.06±0.09
^{9}Be	305.0	180	151±15	1.19±0.08
^{9}Be	346.0	180	188±6	0.96±0.03
^{9}Be	346.0	180	186±6	0.97±0.03
^{9}Be	464.0	180	195±6	0.92±0.03
^{9}Be	464.0	180	189±6	0.95±0.03
^{9}Be	553.0	180	195±6	0.92±0.03
^{9}Be	553.0	180	190±6	0.95±0.03
^{9}Be	860.0	180	169±15	1.06±0.08
B	19.2	576	576±23	1.00±0.04
B	22.2	548	535±19	1.02±0.03
B	24.8	522	509±18	1.03±0.03
B	29.8	474	458±16	1.03±0.03
B	34.8	431	424±13	1.02±0.03
B	39.8	395	388±13	1.02±0.03
B	44.8	365	356±13	1.03±0.04
B	44.8	351	346±13	1.01±0.04
B	235.0	205	197±7	1.04±0.03
B	345.0	205	198±7	1.03±0.03
B	410.0	205	206±6	0.99±0.03
B	497.0	205	210±6	0.98±0.03
B	565.0	205	213±6	0.96±0.03
C	16.2	337	430±16	0.78±0.05
C	16.4	343	368±30	0.93±0.09
C	17.3	378	431±17	0.88±0.04
C	18.6	413	417±17	0.99±0.04
C	19.9	460	438±17	1.05±0.04
C	21.1	454	448±17	1.01±0.04
C	21.8	454	441±21	1.03±0.05
C	22.0	447	420±42	1.06±0.09
C	23.8	434	435±18	1.00±0.04
C	25.0	426	376±40	1.13±0.09
C	25.3	424	416±19	1.02±0.04
C	26.4	417	378±18	1.10±0.04
C	28.0	407	396±13	1.03±0.03
C	29.0	401	418±18	0.96±0.04
C	34.0	375	445±20	0.84±0.05
C	42.0	341	405±35	0.84±0.10
C	54.0	306	355±50	0.86±0.16
C	61.0	290	200±13	1.45±0.04
C	77.0	264	219±8	1.21±0.03
C	95.0	245	232±7	1.06±0.03
C	133.0	221	222±6	0.99±0.03
C	134.0	221	220±24	1.01±0.11
C	180.0	221	212±5	1.04±0.02
C	185.0	221	204±20	1.08±0.09
C	231.0	221	218±5	1.01±0.02
C	231.0	221	215±5	1.02±0.02
C	240.0	221	202±20	1.09±0.09
C	290.0	221	199±20	1.11±0.09
C	305.0	221	187±19	1.18±0.09
C	345.0	221	220±5	1.01±0.02
C	345.0	221	219±5	1.01±0.02
C	464.0	221	232±5	0.95±0.02
C	464.0	221	229±5	0.97±0.02
C	553.0	221	233±5	0.95±0.02
C	553.0	221	229±5	0.97±0.02
C	860.0	221	209±22	1.06±0.10
^{12}C	19.5	445	401±24	1.11±0.05
^{12}C	23.2	439	452±13	0.97±0.03
^{12}C	24.7	428	432±12	0.99±0.03
^{12}C	26.1	419	432±11	0.97±0.03
^{12}C	27.9	407	405±11	1.00±0.03
^{12}C	29.8	396	413±11	0.96±0.03
^{12}C	30.0	395	447±20	0.88±0.05
^{12}C	31.0	390	399±11	0.98±0.03
^{12}C	33.0	379	381±9	0.99±0.02
^{12}C	34.4	372	378±9	0.98±0.02
^{12}C	35.2	369	365±12	1.01±0.03
^{12}C	39.5	350	361±8	0.97±0.02
^{12}C	40.0	348	371±11	0.94±0.03
^{12}C	43.0	338	356±9	0.95±0.03
^{12}C	44.6	332	351±8	0.95±0.02
^{12}C	46.1	327	344±8	0.95±0.02
^{12}C	47.7	322	341±7	0.94±0.02
^{12}C	49.5	317	345±13	0.92±0.04
^{12}C	60.8	290	310±13	0.94±0.04
^{27}Al	16.4	717	701±34	1.02±0.05
^{27}Al	24.8	706	733±20	0.96±0.03
^{27}Al	27.4	693	731±19	0.95±0.03
^{27}Al	29.0	684	775±37	0.88±0.05
^{27}Al	30.4	676	709±18	0.95±0.03
^{27}Al	33.7	657	668±17	0.98±0.03
^{27}Al	34.0	655	600±42	1.09±0.06
^{27}Al	36.9	638	651±16	0.98±0.03
^{27}Al	39.8	622	633±16	0.98±0.03
^{27}Al	40.0	620	645±35	0.96±0.06
^{27}Al	43.2	603	615±16	0.98±0.03
^{27}Al	46.3	588	600±17	0.98±0.03

TABLE I. (*Continued*).

Nucleus	Energy (MeV)	Calculated σ_R (mb)	Experimental σ_R (mb)	$\frac{\sigma(\text{calc})}{\sigma(\text{expt.})}$
^{27}Al	60.8	527	499±27	1.06±0.05
^{27}Al	77.0	480	444±14	1.08±0.03
^{27}Al	95.0	445	415±13	1.07±0.03
^{27}Al	99.7	434	430±12	1.01±0.03
^{27}Al	113.0	402	408±13	0.99±0.03
^{27}Al	133.0	402	424±13	0.95±0.03
^{27}Al	134.0	402	373±37	1.08±0.09
^{27}Al	180.0	402	390±10	1.03±0.02
^{27}Al	185.0	402	408±41	0.99±0.10
^{27}Al	234.0	402	400±7	1.01±0.02
^{27}Al	234.0	402	401±7	1.00±0.02
^{27}Al	240.0	402	383±38	1.05±0.09
^{27}Al	290.0	402	416±42	0.97±0.10
^{27}Al	305.0	402	334±33	1.20±0.08
^{27}Al	348.0[a]	402	402±7	1.00±0.02
^{27}Al	348.0[a]	402	402±7	1.00±0.02
^{27}Al	466.0	402	424±7	0.95±0.02
^{27}Al	466.0	402	421±8	0.96±0.02
^{27}Al	554.0	402	433±8	0.93±0.02
^{27}Al	554.0	402	425±8	0.95±0.02
^{27}Al	860.0	402	394±10	1.02±0.02

[a]Two different measurements.

production of various isotopes of an element of atomic number Z. The Gaussian-like distribution is related to the statistical nature of the nuclear evaporation process [22]. The width of the distribution of cross section is represented by the parameter R. The parameter S describes the location of the peaks of the distribution curves, which go toward greater neutron excess as the atomic number of the product increases.

Silberberg and Tsao [3,23] have constructed a semiempirical equation resembling Rudstam's with additional parameters and have defined regions of target and product mass intervals where these parameters apply. Their basic equation for calculating the partial cross sections is

$$\sigma=\sigma_0 f(A) f(E) e^{-P\Delta A} e^{-R|Z-SA+TA^2|^\nu}\Omega\eta\xi \ . \quad (12)$$

It is applicable for cross sections (in units of mb) of targets having mass numbers in the range $9\leq A_t\leq 209$ and products with $6\leq A\leq 200$, except for peripheral interactions with small values of ΔA (i.e., of A_t-A). For the latter reactions, Silberberg and Tsao constructed a special equation [3]. In Eq. (12), σ_0 is a normalization factor. The factors $f(A)$ and $f(E)$ apply only to products from heavy targets (with atomic numbers $Z_t>30$), when ΔA is large, as for fission, fragmentation, and evaporation of light product nuclei. The factor $\exp(-p\Delta A)$ and the next exponential factor $\exp(-R|Z-SA+TA^2|^\nu)$ have been described above. The parameter Ω is related to the nuclear structure and number of particle-stable levels of a product nuclide. The factor η depends on the pairing of protons and neutrons in the product nucleus; it is largest for even-even nuclei and smallest for odd-odd nuclei. The parameter ζ is introduced to represent the enhancement of light evaporation products.

There are deviations from complete proportionality between proton-nucleus and nucleus-nucleus reactions. The deviations have been explained by Lindstrom *et al.* [24] in terms of (i) nuclear transparency (the energy deposition is less in p-nucleus interactions; so, as ΔA increases, the relative yields of proton-nucleus reactions diminish progressively) and (ii) giant dipole resonance, as a result of which single-nucleon stripping is enhanced in collisions with heavy nuclei. (iii) The lightest products (Li, Be, and B) are also enhanced by a factor of 2–3 beyond the scaling factor for heavier targets [25,26].

Silberberg and Tsao have also developed equations for calculating the cross sections for the breakup of nuclides (Z_i, A_i) colliding with (Z_j, A_j) by scaling their semiempirical systematics [4–6]. However, these equations are based on a first iteration, and to get better agreement with the experimental data, we have constructed a new scaling procedure.

A. Estimation of the scaling factor S_c

In the following we give a prescription how to estimate the scaling factor S_c which is based on a Bradt-Peters-type [8] law and also takes advantage of the weak-factorization property [27] of projectile fragments. The prescription is most valid for projectile energies 600 MeV/nucleon up to 2 GeV/nucleon. A scaling algorithm that is based on the participant-spectator picture of high-energy nucleus-nucleus reactions and also takes advantage of the weak-factorization property mentioned above has also been developed by us [28]. The algorithm allows for the calculation of heavy-ion spallation cross sections by scaling the proton-induced ones in a consistent fashion over the projectile energy range 0.1–2.0 GeV/nucleon with no restrictions (apart from ^{4}He targets) on the mass of the collision system.

Olson *et al.* [27] have found that projectile fragments appear to obey the so-called weak-factorization property expressed as

$$\sigma_f=\gamma_p^f\gamma_{p,t} \ , \quad (13)$$

where σ_f is the partial cross section for the production of the projectile fragment f, γ_p^f is a factor that depends only on the species of the projectile and the fragment, and $\gamma_{p,t}$ is a factor that depends only on the species of the projectile and target. The following relation was found [27] to describe $\gamma_{p,t}$:

$$\gamma_{p,t}=g(A_p^{1/3}+A_t^{1/3}-\delta) \ , \quad (14)$$

where g and δ are free parameters. Scaling to proton-nucleus cross sections in our procedure essentially means

$$S_C\rightarrow\gamma_{p,t} \ . \quad (15)$$

Semiempirical expressions for g and δ can be written as

$$g=(1+A_t^{1/3}-b_0^{(pN)})^{-1} \quad (16)$$

and

$$\delta=b_0^{(NN)} \ , \quad (17)$$

where $b_0^{(pN)}$ and $b_0^{(NN)}$ are the overlap parameters $b_0(1+A_t^{-1/3})$ for the proton-nucleus reactions in Eqs. (4) and (5) and $b_0(A_p^{-1/3}+A_t^{-1/3})$ for nucleus-nucleus reactions in Eqs. (9) and (10), respectively. It is interesting to note the correspondence between b_0 in Eq. (2) and δ above. This is consistent with the parametrization of Olson *et al.* [27] of δ as a relative measure of the overlap of target and projectile nuclei, which contributes to peripheral fragmentation. The parameter g, however, is not so easily identifiable with the geometric parameters of the collision. It appears to be specific to the scaling procedure, i.e., to the proton-nucleus cross sections in ours. Thus we identify g as a scaling-specific parameter, while δ as a geometric overlap parameter.

B. Calculation of the partial nucleus-nucleus cross sections

The scaling of the proton-nucleus partial cross sections is done by the scaling parameter S_c, described in the previous section, and additional enhancement factors. Since our total reaction cross section formulas include the transparency function, our scaling takes into account that the energy deposition is less in p-nucleus interactions than in nucleus-nucleus interactions. Our equation for calculating the cross sections for the breakup of nuclides (Z_i, A_i) colliding with (Z_j, A_j) is

$$\sigma(Z_i, A_i, Z_j A_j, E_i) = S_C \varepsilon_L \varepsilon_\Delta \varepsilon_1 \sigma(Z_i, A_i, p, E_p) , \quad (18)$$

where S_c, as described in Eq. (15), is equivalent to the expression described by Sihver and Kanai [1] and $\sigma(Z_i, A_i, Z_j, A_j, E_i)$ is the partial cross section of nucleus-nucleus reactions, for the breakup of nuclides (A_i, Z_i, E_i) colliding with (A_j, Z_j), $\sigma(Z_i, A_i, p, E_p)$ is the partial cross section of proton-nucleus reactions, for the breakup of nuclides (A_i, Z_i) colliding with protons (E_p), ε_L is the enhancement factor for the lightest products Li, Be, and B, ε_Δ is the enhancement factor for reactions with a large value of ΔA, and ε_1 is the enhancement factor for single-nucleon stripping, caused by the giant dipole resonance. The enhancement factors for the lightest products are the following: (A) For $E_i \leq 1100$ MeV/nucleon and $Z_p \geq 8$,

$$\varepsilon_L = [1+0.7 f_B] f_A . \quad (19)$$

(B) For $E_i > 2000$ MeV/nucleon, $Z_p \geq 8$, and $3 \leq Z_{\text{frag}} \leq 5$,

$$\varepsilon_L = \left\{ 1+\left[1+\left[\frac{5-Z_{\text{frag}}}{10}\right]\right]\left[\frac{1}{2Z_{\text{frag}}}\right] \right\} f_B . \quad (20)$$

There are no experimental data in the region 1100–2000 MeV/nucleon, and so the enhancement factor in this region is not known. As a first approximation, a linear fitting between Eqs. (19) and (20) can be made in this region. The enhancement factor for reactions with a large value of ΔA is

$$\varepsilon_\Delta = 4 f_A e^{-2.2 A_{\text{frag}}/A_i} , \quad (21)$$

for $E_i \leq 2000$ MeV/nucleon, $A_{\text{frag}} < A_p/2$, and $Z_{\text{frag}} > 5$, where

$$f_A = \frac{[1+(A_i/120)(E_i/2000)]}{[1+(A_i/120)]} \quad (22)$$

and

$$f_B = \left[1+0.03\left[\frac{Z_i}{Z_{\text{frag}}}\right]^2\right]\left[1-1.5\left[\frac{Z_{\text{frag}}}{Z_i}\right]\right] , \quad (23)$$

where Z_{frag} and A_{frag} are the atomic and mass numbers of the projectile fragment, respectively.

The enhancement factor for single-nucleon stripping caused by the giant dipole resonance is

$$\varepsilon_1 = 1+0.0088 Z_i Z_j^{0.8} \text{ for } Z_i \geq 8, \ \Delta A = 1 , \quad (24)$$

and

$$\varepsilon_1 = 1 \text{ for } Z_i < 8 , \ \Delta A = 1 . \quad (25)$$

We have also introduced the following correction factors: $\sigma(^8\text{B})$ is enhanced with the factor 2.4, $\sigma(^9\text{C})$ with the factor 2.1, and $\sigma(^{12}\text{N})$ with the factor 0.6. $\sigma(^6\text{Li})$ is enhanced with the factor 1.2 for $E > 2000$ MeV/nucleon and $Z_p \geq 8$.

The energy dependence scales to nucleus-proton cross sections approximately as the energy per nucleus of the nucleus A_j in the rest frame of A, e.g., for ^{16}O at 200 MeV/nucleon incident on ^{12}C, the cross section scales to the $A_j - p$ cross section at $200 \times 12 = 2400$ MeV [4]. All products from the Z of the projectile down to $Z=2$ can be calculated. In Table II the calculated partial nucleus-nucleus cross sections are tabulated, together with the experimental data, for all studied reactions. Figure 4 shows

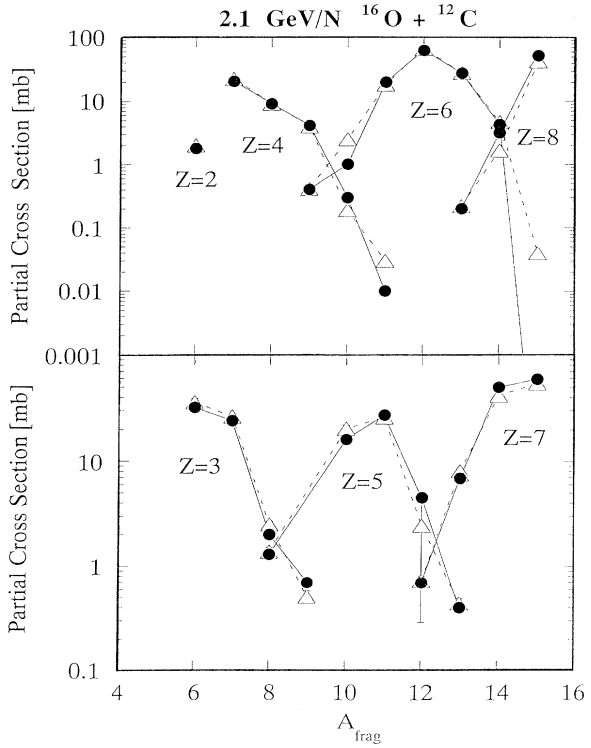

FIG. 4. Calculated partial nucleus-nucleus cross sections for the reaction of 2.1 GeV/nucleon ^{16}O with ^{12}C, together with the experimental data from Ref. [27]. The solid circles are the calculated values, and the open circles are the experimental data. When only a solid circle can be seen, the calculated value "is in coincidence with the experimental data point."

TABLE II. Calculated projectile fragmentation cross sections, together with experimental data.

Reaction	Fragment Z, A	Expt. cross section (mb)	Calc. cross section (mb)	Ref.
250 MeV/nucl. $^{12}C+^{12}C$	6,11	55.97±4.06	53.3	[29]
250 MeV/nucl. $^{12}C+^{12}C$	6,10	5.33±0.81	2.3	[29]
250 MeV/nucl. $^{12}C+^{12}C$	5,12	0.49±1.00	0.0	[29]
250 MeV/nucl. $^{12}C+^{12}C$	5,11	65.61±2.55	62.5	[29]
250 MeV/nucl. $^{12}C+^{12}C$	5,10	47.50±2.42	34.4	[29]
250 MeV/nucl. $^{12}C+^{12}C$	5,8	3.21±1.20	1.5	[29]
250 MeV/nucl. $^{12}C+^{12}C$	4,11	0.36±0.26	0.0	[29]
250 MeV/nucl. $^{12}C+^{12}C$	4,10	5.88±9.70	4.6	[29]
250 MeV/nucl. $^{12}C+^{12}C$	4,9	10.44±0.85	6.8	[29]
250 MeV/nucl. $^{12}C+^{12}C$	4,7	22.64±1.49	15.4	[29]
250 MeV/nucl. $^{12}C+^{12}C$	3,8	1.33±1.00	1.5	[29]
250 MeV/nucl. $^{12}C+^{12}C$	3,7	17.19±3.00	18.0	[29]
250 MeV/nucl. $^{12}C+^{12}C$	3,6	26.35±2.10	20.0	[29]
600 MeV/nucl. $^{12}C+^{12}C$	6,11	53.6[a]	53.3	[30]
600 MeV/nucl. $^{12}C+^{12}C$	6,10	2.1[b]	2.3	[30]
600 MeV/nucl. $^{12}C+^{12}C$	5,11	70.7[a]	62.5	[30]
600 MeV/nucl. $^{12}C+^{12}C$	5,10	38.6[a]	34.4	[30]
600 MeV/nucl. $^{12}C+^{12}C$	4,10	5.6[b]	5.7	[30]
600 MeV/nucl. $^{12}C+^{12}C$	4,9	9.6[c]	8.4	[30]
600 MeV/nucl. $^{12}C+^{12}C$	4,7	15.5[c]	19.2	[30]
600 MeV/nucl. $^{14}N+^{12}C$	7,13	13.3[c]	20.6	[30]
600 MeV/nucl. $^{14}N+^{12}C$	7,12	2.0[d]	1.5	[30]
600 MeV/nucl. $^{14}N+^{12}C$	6,13	21.3[a]	20.3	[30]
600 MeV/nucl. $^{14}N+^{12}C$	6,12	117.2[a]	73.6	[30]
600 MeV/nucl. $^{14}N+^{12}C$	6,11	7.5[a]	23.9	[30]
600 MeV/nucl. $^{14}N+^{12}C$	6,10	2.1[d]	1.2	[30]
600 MeV/nucl. $^{14}N+^{12}C$	5,11	39.8[d]	29.1	[30]
600 MeV/nucl. $^{14}N+^{12}C$	5,10	23.9[a]	31.0	[30]
600 MeV/nucl. $^{14}N+^{12}C$	4,10	3.5[d]	3.7	[30]
600 MeV/nucl. $^{14}N+^{12}C$	4,9	4.1[d]	8.2	[30]
600 MeV/nucl. $^{14}N+^{12}C$	4,7	21.6[c]	18.7	[30]
600 MeV/nucl. $^{16}O+^{12}C$	8,15	84.0[a]	68.2	[30]
600 MeV/nucl. $^{16}O+^{12}C$	8,14	2.6[d]	3.2	[30]
600 MeV/nucl. $^{16}O+^{12}C$	7,15	73.2[a]	77.2	[30]
600 MeV/nucl. $^{16}O+^{12}C$	7,14	66.8[a]	49.8	[30]
600 MeV/nucl. $^{16}O+^{12}C$	7,13	12.6[c]	6.9	[30]
600 MeV/nucl. $^{16}O+^{12}C$	7,12	0.6[d]	0.7	[30]
600 MeV/nucl. $^{16}O+^{12}C$	6,14	3.3[b]	4.3	[30]
600 MeV/nucl. $^{16}O+^{12}C$	6,13	41.0[a]	27.2	[30]
600 MeV/nucl. $^{16}O+^{12}C$	6,12	79.2[a]	61.8	[30]
600 MeV/nucl. $^{16}O+^{12}C$	6,11	26.5[a]	20.1	[30]
600 MeV/nucl. $^{16}O+^{12}C$	6,10	3.2[d]	1.0	[30]
600 MeV/nucl. $^{16}O+^{12}C$	5,12	2.4[d]	6.9	[30]
600 MeV/nucl. $^{16}O+^{12}C$	5,11	36.0[a]	41.6	[30]
600 MeV/nucl. $^{16}O+^{12}C$	5,10	24.8[a]	24.7	[30]
600 MeV/nucl. $^{40}Ar+^{12}C$	18,39	146.4[a]	118.4	[30]
600 MeV/nucl. $^{40}Ar+^{12}C$	18,38	72.3[a]	19.2	[30]
600 MeV/nucl. $^{40}Ar+^{12}C$	18,37	8.4[b]	2.5	[30]
600 MeV/nucl. $^{40}Ar+^{12}C$	17,39	39.1[a]	41.3	[30]
600 MeV/nucl. $^{40}Ar+^{12}C$	17,38	34.9[a]	25.1	[30]
600 MeV/nucl. $^{40}Ar+^{12}C$	17,37	59.3[a]	28.0	[30]
600 MeV/nucl. $^{40}Ar+^{12}C$	17,36	38.0[a]	33.7	[30]
600 MeV/nucl. $^{40}Ar+^{12}C$	17,35	12.3[b]	19.7	[30]
600 MeV/nucl. $^{40}Ar+^{12}C$	16,38	0.8[d]	0.7	[30]
600 MeV/nucl. $^{40}Ar+^{12}C$	16,37	5.1[b]	3.6	[30]
600 MeV/nucl. $^{40}Ar+^{12}C$	16,36	19.3[c]	20.0	[30]
600 MeV/nucl. $^{40}Ar+^{12}C$	16,35	32.6[a]	30.1	[30]

TABLE II. (*Continued*).

Reaction	Fragment Z, A	Expt. cross section (mb)	Calc. cross section (mb)	Ref.
600 MeV/nucl. $^{40}Ar+^{12}C$	16,34	51.0[a]	45.8	[30]
600 MeV/nucl. $^{40}Ar+^{12}C$	16,33	15.3[c]	18.9	[30]
600 MeV/nucl. $^{40}Ar+^{12}C$	16,32	1.1[d]	7.8	[30]
600 MeV/nucl. $^{40}Ar+^{12}C$	15,35	1.2[d]	2.3	[30]
600 MeV/nucl. $^{40}Ar+^{12}C$	15,34	6.3[b]	9.1	[30]
600 MeV/nucl. $^{40}Ar+^{12}C$	15,33	23.8[a]	25.9	[30]
600 MeV/nucl. $^{40}Ar+^{12}C$	15,32	35.9[a]	27.9	[30]
600 MeV/nucl. $^{40}Ar+^{12}C$	15,31	24.0[a]	21.6	[30]
600 MeV/nucl. $^{40}Ar+^{12}C$	15,30	2.2[d]	6.2	[30]
600 MeV/nucl. $^{40}Ar+^{12}C$	14,32	4.1[b]	8.7	[30]
600 MeV/nucl. $^{40}Ar+^{12}C$	14,31	17.6[c]	17.6	[30]
600 MeV/nucl. $^{40}Ar+^{12}C$	14,30	40.1[a]	35.5	[30]
600 MeV/nucl. $^{40}Ar+^{12}C$	14,29	27.6[a]	19.2	[30]
600 MeV/nucl. $^{40}Ar+^{12}C$	14,28	9.2[b]	10.3	[30]
600 MeV/nucl. $^{40}Ar+^{12}C$	13,30	1.2[d]	3.8	[30]
600 MeV/nucl. $^{40}Ar+^{12}C$	13,29	11.8[c]	14.5	[30]
600 MeV/nucl. $^{40}Ar+^{12}C$	13,28	20.5[a]	20.4	[30]
600 MeV/nucl. $^{40}Ar+^{12}C$	13,27	33.1[a]	20.5	[30]
600 MeV/nucl. $^{40}Ar+^{12}C$	13,26	4.2[d]	7.6	[30]
600 MeV/nucl. $^{40}Ar+^{12}C$	12,27	4.1[b]	9.5	[30]
600 MeV/nucl. $^{40}Ar+^{12}C$	12,26	23.0[a]	24.8	[30]
600 MeV/nucl. $^{40}Ar+^{12}C$	12,25	23.1[a]	17.3	[30]
600 MeV/nucl. $^{40}Ar+^{12}C$	12,24	12.7[c]	11.8	[30]
600 MeV/nucl. $^{40}Ar+^{12}C$	12,23	1.0[d]	2.1	[30]
600 MeV/nucl. $^{56}Fe+^{12}C$	26,55	164.3[a]	159.9	[30]
600 MeV/nucl. $^{56}Fe+^{12}C$	26,54	28.2[c]	23.7	[30]
600 MeV/nucl. $^{56}Fe+^{12}C$	26,53	3.0[d]	5.2	[30]
600 MeV/nucl. $^{56}Fe+^{12}C$	25,55	53.7[a]	123.2	[30]
600 MeV/nucl. $^{56}Fe+^{12}C$	25,54	66.9[a]	71.6	[30]
600 MeV/nucl. $^{56}Fe+^{12}C$	25,53	64.0[a]	42.6	[30]
600 MeV/nucl. $^{56}Fe+^{12}C$	25,52	21.6[c]	10.2	[30]
600 MeV/nucl. $^{56}Fe+^{12}C$	25,51	3.9[d]	2.5	[30]
600 MeV/nucl. $^{56}Fe+^{12}C$	24,54	4.7[b]	4.7	[30]
600 MeV/nucl. $^{56}Fe+^{12}C$	24,53	16.0[c]	14.9	[30]
600 MeV/nucl. $^{56}Fe+^{12}C$	24,52	63.6[a]	47.5	[30]
600 MeV/nucl. $^{56}Fe+^{12}C$	24,51	60.7[a]	32.3	[30]
600 MeV/nucl. $^{56}Fe+^{12}C$	24,50	30.5[a]	17.1	[30]
600 MeV/nucl. $^{56}Fe+^{12}C$	24,49	5.1[b]	2.8	[30]
600 MeV/nucl. $^{56}Fe+^{12}C$	23,52	1.1[d]	1.2	[30]
600 MeV/nucl. $^{56}Fe+^{12}C$	23,51	8.3[b]	5.5	[30]
600 MeV/nucl. $^{56}Fe+^{12}C$	23,50	33.1[a]	16.7	[30]
600 MeV/nucl. $^{56}Fe+^{12}C$	23,49	43.0[a]	29.5	[30]
600 MeV/nucl. $^{56}Fe+^{12}C$	23,48	24.7[a]	11.8	[30]
600 MeV/nucl. $^{56}Fe+^{12}C$	23,47	4.9[d]	3.8	[30]
600 MeV/nucl. $^{56}Fe+^{12}C$	22,50	1.6[d]	2.9	[30]
600 MeV/nucl. $^{56}Fe+^{12}C$	22,49	8.4[b]	6.6	[30]
600 MeV/nucl. $^{56}Fe+^{12}C$	22,48	30.5[a]	26.2	[30]
600 MeV/nucl. $^{56}Fe+^{12}C$	22,47	40.6[a]	31.0	[30]
600 MeV/nucl. $^{56}Fe+^{12}C$	22,46	23.3[a]	20.3	[30]
600 MeV/nucl. $^{56}Fe+^{12}C$	22,45	4.0[d]	4.1	[30]
600 MeV/nucl. $^{56}Fe+^{12}C$	22,44	0.6[d]	0.8	[30]
600 MeV/nucl. $^{56}Fe+^{12}C$	21,48	0.3[d]	1.2	[30]
600 MeV/nucl. $^{56}Fe+^{12}C$	21,47	2.7[d]	4.8	[30]
600 MeV/nucl. $^{56}Fe+^{12}C$	21,46	12.8[c]	13.0	[30]
600 MeV/nucl. $^{56}Fe+^{12}C$	21,45	28.3[a]	30.7	[30]
600 MeV/nucl. $^{56}Fe+^{12}C$	21,44	21.5[a]	15.0	[30]
600 MeV/nucl. $^{56}Fe+^{12}C$	21,43	6.9[b]	5.2	[30]
600 MeV/nucl. $^{56}Fe+^{12}C$	20,45	2.7[d]	2.9	[30]

TABLE II. (*Continued*).

Reaction	Fragment Z, A	Expt. cross section (mb)	Calc. cross section (mb)	Ref.
600 MeV/nucl. $^{56}Fe+^{12}C$	20,44	10.6[c]	13.7	[30]
600 MeV/nucl. $^{56}Fe+^{12}C$	20,43	22.6[a]	22.8	[30]
600 MeV/nucl. $^{56}Fe+^{12}C$	20,42	22.0[a]	23.6	[30]
600 MeV/nucl. $^{56}Fe+^{12}C$	20,41	10.9[b]	5.4	[30]
600 MeV/nucl. $^{56}Fe+^{12}C$	20,40	1.3[d]	1.3	[30]
600 MeV/nucl. $^{56}Fe+^{12}C$	19,44	0.7[d]	0.5	[30]
600 MeV/nucl. $^{56}Fe+^{12}C$	19,43	2.8[d]	2.1	[30]
600 MeV/nucl. $^{56}Fe+^{12}C$	19,42	8.1[b]	6.5	[30]
600 MeV/nucl. $^{56}Fe+^{12}C$	19,41	16.6[c]	20.2	[30]
600 MeV/nucl. $^{56}Fe+^{12}C$	19,40	14.6[c]	16.7	[30]
600 MeV/nucl. $^{56}Fe+^{12}C$	19,39	7.3[b]	6.8	[30]
600 MeV/nucl. $^{56}Fe+^{12}C$	19,38	1.0[d]	1.2	[30]
600 MeV/nucl. $^{56}Fe+^{12}C$	18,41	1.7[d]	1.3	[30]
600 MeV/nucl. $^{56}Fe+^{12}C$	18,40	8.0[b]	6.6	[30]
600 MeV/nucl. $^{56}Fe+^{12}C$	18,39	17.9[c]	14.1	[30]
600 MeV/nucl. $^{56}Fe+^{12}C$	18,38	19.1[c]	25.2	[30]
600 MeV/nucl. $^{56}Fe+^{12}C$	18,37	6.1[b]	7.0	[30]
600 MeV/nucl. $^{56}Fe+^{12}C$	18,36	1.1[d]	2.3	[30]
600 MeV/nucl. $^{56}Fe+^{12}C$	17,39	0.9[d]	0.9	[30]
600 MeV/nucl. $^{56}Fe+^{12}C$	17,38	3.4[d]	2.9	[30]
600 MeV/nucl. $^{56}Fe+^{12}C$	17,37	12.5[c]	10.9	[30]
600 MeV/nucl. $^{56}Fe+^{12}C$	17,36	13.5[c]	15.2	[30]
600 MeV/nucl. $^{56}Fe+^{12}C$	17,35	9.6[b]	7.8	[30]
600 MeV/nucl. $^{56}Fe+^{12}C$	17,34	0.9[d]	1.7	[30]
600 MeV/nucl. $^{56}Fe+^{12}C$	16,37	0.6[d]	0.6	[30]
600 MeV/nucl. $^{56}Fe+^{12}C$	16,36	2.2[d]	3.3	[30]
600 MeV/nucl. $^{56}Fe+^{12}C$	16,35	8.0[b]	8.3	[30]
600 MeV/nucl. $^{56}Fe+^{12}C$	16,34	14.6[c]	22.9	[30]
600 MeV/nucl. $^{56}Fe+^{12}C$	16,33	11.1[c]	8.5	[30]
600 MeV/nucl. $^{56}Fe+^{12}C$	16,32	5.6[b]	3.5	[30]
600 MeV/nucl. $^{56}Fe+^{12}C$	16,31	1.6[d]	0.4	[30]
1.05 GeV/nucl. $^{12}C+^{9}Be$	7,12	0.02±0.01	0.05	[27]
1.05 GeV/nucl. $^{12}C+^{9}Be$	6,11	44.7±2.6	50.4	[27]
1.05 GeV/nucl. $^{12}C+^{9}Be$	6,10	4.02±0.23	2.2	[27]
1.05 GeV/nucl. $^{12}C+^{9}Be$	6,9	0.42±0.05	0.6	[27]
1.05 GeV/nucl. $^{12}C+^{9}Be$	5,12	0.09±0.02	0.0	[27]
1.05 GeV/nucl. $^{12}C+^{9}Be$	5,11	50.7±3.2	59.1	[27]
1.05 GeV/nucl. $^{12}C+^{9}Be$	5,10	28.8±2.3	32.5	[27]
1.05 GeV/nucl. $^{12}C+^{9}Be$	5,8	1.55±0.08	1.4	[27]
1.05 GeV/nucl. $^{12}C+^{9}Be$	4,11	0.02±0.01	0.0	[27]
1.05 GeV/nucl. $^{12}C+^{9}Be$	4,10	5.08±0.30	5.4	[27]
1.05 GeV/nucl. $^{12}C+^{9}Be$	4,9	11.60±0.76	8.0	[27]
1.05 GeV/nucl. $^{12}C+^{9}Be$	4,7	17.80±0.90	18.2	[27]
1.05 GeV/nucl. $^{12}C+^{9}Be$	3,9	0.75±0.08	0.7	[27]
1.05 GeV/nucl. $^{12}C+^{9}Be$	3,8	2.36±0.14	1.7	[27]
1.05 GeV/nucl. $^{12}C+^{9}Be$	3,7	23.4±1.2	21.3	[27]
1.05 GeV/nucl. $^{12}C+^{9}Be$	3,6	24.8±2.0	23.6	[27]
1.05 GeV/nucl. $^{12}C+^{9}Be$	2,6	2.09±0.17	1.5	[27]
1.05 GeV/nucl. $^{12}C+^{12}C$	7,12	0.05	0.05	[27]
1.05 GeV/nucl. $^{12}C+^{12}C$	6,11	44.7±2.8	53.3	[27]
1.05 GeV/nucl. $^{12}C+^{12}C$	6,10	4.44±0.24	2.3	[27]
1.05 GeV/nucl. $^{12}C+^{12}C$	6,9	0.48±0.06	0.6	[27]
1.05 GeV/nucl. $^{12}C+^{12}C$	5,12	0.10±0.01	0.0	[27]
1.05 GeV/nucl. $^{12}C+^{12}C$	5,11	48.6±2.4	62.5	[27]
1.05 GeV/nucl. $^{12}C+^{12}C$	5,10	27.9±2.2	34.4	[27]
1.05 GeV/nucl. $^{12}C+^{12}C$	5,8	1.43±0.10	1.5	[27]
1.05 GeV/nucl. $^{12}C+^{12}C$	4,10	5.34±0.29	5.7	[27]
1.05 GeV/nucl. $^{12}C+^{12}C$	4,9	10.70±0.50	8.4	[27]

TABLE II. (*Continued*).

Reaction	Fragment Z, A	Expt. cross section (mb)	Calc. cross section (mb)	Ref.
1.05 GeV/nucl. $^{12}C+^{12}C$	4,7	18.60±0.90	19.2	[27]
1.05 GeV/nucl. $^{12}C+^{12}C$	3,9	0.87±0.01	0.7	[27]
1.05 GeV/nucl. $^{12}C+^{12}C$	3,8	2.40±0.18	1.8	[27]
1.05 GeV/nucl. $^{12}C+^{12}C$	3,7	21.5±1.1	22.6	[27]
1.05 GeV/nucl. $^{12}C+^{12}C$	3,6	27.1±2.2	25.0	[27]
1.05 GeV/nucl. $^{12}C+^{12}C$	2,6	1.83±0.19	1.5	[27]
1.05 GeV/nucl. $^{12}C+^{27}Al$	7,12	6.49±0.48	0.06	[27]
1.05 GeV/nucl. $^{12}C+^{27}Al$	6,11	57.8±3.9	63.3	[27]
1.05 GeV/nucl. $^{12}C+^{27}Al$	6,10	5.06±0.37	2.8	[27]
1.05 GeV/nucl. $^{12}C+^{27}Al$	6,9	0.60±0.10	0.7	[27]
1.05 GeV/nucl. $^{12}C+^{27}Al$	5,12	0.18±0.05	0.0	[27]
1.05 GeV/nucl. $^{12}C+^{27}Al$	5,11	64.5±5.3	74.2	[27]
1.05 GeV/nucl. $^{12}C+^{27}Al$	5,10	30.4±3.5	40.8	[27]
1.05 GeV/nucl. $^{12}C+^{27}Al$	5,8	1.73±0.16	1.8	[27]
1.05 GeV/nucl. $^{12}C+^{27}Al$	4,10	6.49±0.48	6.8	[27]
1.05 GeV/nucl. $^{12}C+^{27}Al$	4,9	13.90±0.90	10.0	[27]
1.05 GeV/nucl. $^{12}C+^{27}Al$	4,7	19.9±1.1	22.8	[27]
1.05 GeV/nucl. $^{12}C+^{27}Al$	3,9	0.82±0.16	0.8	[27]
1.05 GeV/nucl. $^{12}C+^{27}Al$	3,8	2.87±0.27	2.2	[27]
1.05 GeV/nucl. $^{12}C+^{27}Al$	3,7	28.5±1.4	26.8	[27]
1.05 GeV/nucl. $^{12}C+^{27}Al$	3,6	24.9±2.9	29.7	[27]
1.05 GeV/nucl. $^{12}C+^{27}Al$	2,6	2.00±0.29	1.8	[27]
2.1 GeV/nucl. $^{12}C+^{9}Be$	7,12	0.06±0.01	0.05	[27]
2.1 GeV/nucl. $^{12}C+^{9}Be$	6,11	46.7±2.3	50.4	[27]
2.1 GeV/nucl. $^{12}C+^{9}Be$	6,10	4.20±0.21	2.2	[27]
2.1 GeV/nucl. $^{12}C+^{9}Be$	6,9	0.54±0.06	0.6	[27]
2.1 GeV/nucl. $^{12}C+^{9}Be$	5,12	0.14±0.02	0.0	[27]
2.1 GeV/nucl. $^{12}C+^{9}Be$	5,11	53.2±2.9	59.1	[27]
2.1 GeV/nucl. $^{12}C+^{9}Be$	5,10	31.1±2.6	32.5	[27]
2.1 GeV/nucl. $^{12}C+^{9}Be$	5,8	1.48±0.09	1.4	[27]
2.1 GeV/nucl. $^{12}C+^{9}Be$	4,11	0.02±0.01	0.0	[27]
2.1 GeV/nucl. $^{12}C+^{9}Be$	4,10	5.97±0.31	5.4	[27]
2.1 GeV/nucl. $^{12}C+^{9}Be$	4,9	10.98±0.55	8.0	[27]
2.1 GeV/nucl. $^{12}C+^{9}Be$	4,7	18.91±0.95	18.2	[27]
2.1 GeV/nucl. $^{12}C+^{9}Be$	3,9	0.92±0.08	0.7	[27]
2.1 GeV/nucl. $^{12}C+^{9}Be$	3,8	2.52±0.16	1.7	[27]
2.1 GeV/nucl. $^{12}C+^{9}Be$	3,7	22.8±1.1	21.3	[27]
2.1 GeV/nucl. $^{12}C+^{9}Be$	3,6	33.1±2.7	28.3	[27]
2.1 GeV/nucl. $^{12}C+^{9}Be$	2,6	2.54±0.25	1.5	[27]
2.1 GeV/nucl. $^{12}C+^{12}C$	7,12	0.08±0.01	0.05	[27]
2.1 GeV/nucl. $^{12}C+^{12}C$	6,11	46.5±2.3	53.3	[27]
2.1 GeV/nucl. $^{12}C+^{12}C$	6,10	4.11±0.22	2.3	[27]
2.1 GeV/nucl. $^{12}C+^{12}C$	6,9	0.54±0.07	0.6	[27]
2.1 GeV/nucl. $^{12}C+^{12}C$	5,12	0.10±0.01	0.0	[27]
2.1 GeV/nucl. $^{12}C+^{12}C$	5,11	53.8±2.7	62.5	[27]
2.1 GeV/nucl. $^{12}C+^{12}C$	5,10	35.1±3.4	34.4	[27]
2.1 GeV/nucl. $^{12}C+^{12}C$	5,8	1.72±0.13	1.5	[27]
2.1 GeV/nucl. $^{12}C+^{12}C$	4,10	5.81±0.29	5.7	[27]
2.1 GeV/nucl. $^{12}C+^{12}C$	4,9	10.63±0.53	8.4	[27]
2.1 GeV/nucl. $^{12}C+^{12}C$	4,7	18.61±0.93	19.2	[27]
2.1 GeV/nucl. $^{12}C+^{12}C$	3,9	0.85±0.08	0.7	[27]
2.1 GeV/nucl. $^{12}C+^{12}C$	3,8	2.18±0.15	1.8	[27]
2.1 GeV/nucl. $^{12}C+^{12}C$	3,7	21.5±1.1	22.6	[27]
2.1 GeV/nucl. $^{12}C+^{12}C$	3,6	30.0±2.4	30.0	[27]
2.1 GeV/nucl. $^{12}C+^{12}C$	2,6	2.21±0.22	1.5	[27]
2.1 GeV/nucl. $^{12}C+^{27}Al$	6,11	59.5±3.1	63.3	[27]
2.1 GeV/nucl. $^{12}C+^{27}Al$	6,10	4.99±0.34	2.8	[27]

TABLE II. (*Continued*).

Reaction	Fragment Z, A	Expt. cross section (mb)	Calc. cross section (mb)	Ref.
2.1 GeV/nucl. $^{12}C+^{27}Al$	6,9	0.50±0.09	0.7	[27]
2.1 GeV/nucl. $^{12}C+^{27}Al$	5,12	0.14±0.03	0.0	[27]
2.1 GeV/nucl. $^{12}C+^{27}Al$	5,11	65.2±4.8	74.2	[27]
2.1 GeV/nucl. $^{12}C+^{27}Al$	5,10	36.4±4.8	40.8	[27]
2.1 GeV/nucl. $^{12}C+^{27}Al$	5,8	1.76±0.14	1.8	[27]
2.1 GeV/nucl. $^{12}C+^{27}Al$	4,10	7.02±0.40	6.8	[27]
2.1 GeV/nucl. $^{12}C+^{27}Al$	4,9	12.74±0.71	10.0	[27]
2.1 GeV/nucl. $^{12}C+^{27}Al$	4,7	25.8±1.3	22.8	[27]
2.1 GeV/nucl. $^{12}C+^{27}Al$	3,9	0.88±0.12	0.8	[27]
2.1 GeV/nucl. $^{12}C+^{27}Al$	3,8	2.79±0.23	2.2	[27]
2.1 GeV/nucl. $^{12}C+^{27}Al$	3,7	27.3±1.4	26.8	[27]
2.1 GeV/nucl. $^{12}C+^{27}Al$	3,6	36.3±2.9	35.6	[27]
2.1 GeV/nucl. $^{12}C+^{27}Al$	2,6	2.82±0.27	1.8	[27]
2.1 GeV/nucl. $^{16}O+^{12}C$	8,15	42.9±2.3	52.7	[27]
2.1 GeV/nucl. $^{16}O+^{12}C$	8,14	1.67±0.12	3.2	[27]
2.1 GeV/nucl. $^{16}O+^{12}C$	8,13	0.22±0.03	0.2	[27]
2.1 GeV/nucl. $^{16}O+^{12}C$	7,15	54.2±2.9	59.6	[27]
2.1 GeV/nucl. $^{16}O+^{12}C$	7,14	41.8±3.3	49.8	[27]
2.1 GeV/nucl. $^{16}O+^{12}C$	7,13	8.06±0.42	6.9	[27]
2.1 GeV/nucl. $^{16}O+^{12}C$	7,12	0.73±0.07	0.7	[27]
2.1 GeV/nucl. $^{16}O+^{12}C$	6,15	0.04±0.01	0.0	[27]
2.1 GeV/nucl. $^{16}O+^{12}C$	6,14	4.71±0.31	4.3	[27]
2.1 GeV/nucl. $^{16}O+^{12}C$	6,13	27.7±1.4	27.2	[27]
2.1 GeV/nucl. $^{16}O+^{12}C$	6,12	65.1±5.2	61.8	[27]
2.1 GeV/nucl. $^{16}O+^{12}C$	6,11	18.46±0.92	20.1	[27]
2.1 GeV/nucl. $^{16}O+^{12}C$	6,10	2.51±0.16	1.0	[27]
2.1 GeV/nucl. $^{16}O+^{12}C$	6,9	0.41±0.09	0.4	[27]
2.1 GeV/nucl. $^{16}O+^{12}C$	5,13	0.44±0.05	0.4	[27]
2.1 GeV/nucl. $^{16}O+^{12}C$	5,12	2.44±2.15	4.5	[27]
2.1 GeV/nucl. $^{16}O+^{12}C$	5,11	26.0±1.3	27.2	[27]
2.1 GeV/nucl. $^{16}O+^{12}C$	5,10	20.3±1.6	16.1	[27]
2.1 GeV/nucl. $^{16}O+^{12}C$	5,8	1.38±0.13	1.3	[27]
2.1 GeV/nucl. $^{16}O+^{12}C$	4,12	0.03±0.02	0.01	[27]
2.1 GeV/nucl. $^{16}O+^{12}C$	4,11	0.19±0.03	0.3	[27]
2.1 GeV/nucl. $^{16}O+^{12}C$	4,10	3.98±0.30	4.1	[27]
2.1 GeV/nucl. $^{16}O+^{12}C$	4,9	9.06±0.51	9.0	[27]
2.1 GeV/nucl. $^{16}O+^{12}C$	4,7	22.3±1.1	20.5	[27]
2.1 GeV/nucl. $^{16}O+^{12}C$	3,9	0.51±0.07	0.7	[27]
2.1 GeV/nucl. $^{16}O+^{12}C$	3,8	2.50±0.18	2.0	[27]
2.1 GeV/nucl. $^{16}O+^{12}C$	3,7	26.3±1.3	24.1	[27]
2.1 GeV/nucl. $^{16}O+^{12}C$	3,6	35.9±2.9	32.1	[27]
2.1 GeV/nucl. $^{16}O+^{12}C$	2,6	2.00±0.21	1.8	[27]

[a]±1.5% error.
[b]±5% error.
[c]±3% error.
[d]±10% error.

the calculated partial nucleus-nucleus cross sections for the reaction of 2.1 GeV/nucleon ^{16}O with ^{12}C, together with the experimental data, as a typical example.

IV. SUMMARY

We have developed semiempirical total reaction cross section formulas for proton-nucleus (with $Z_t \leq 26$) and nucleus-nucleus (with Z_p and $Z_t \leq 26$) reactions. These formulas apply for incident energies above ≈ 15 MeV and ≈ 100 MeV/nucleon, respectively. For the nucleus-nucleus total reaction cross sections, we have assumed energy independence for incident energies above 100 MeV/nucleon, and for the proton-nucleus reaction cross sections we assumed energy independence above 200 MeV.

We have also constructed a procedure for calculating the projectile fragment production cross sections, by scaling semiempirical proton-nucleus partial cross section systematics. The scaling is done by a scaling parameter,

which is based on a Bradt-Peters-type [8] law and takes advantage of the weak-factorization property [27] of projectile fragments. All products from the Z of the projectile down to $Z=2$ can be calculated with our procedure. The agreement between the calculated partial cross sections and the experimental data is better than all earlier published results.

ACKNOWLEDGMENTS

One of us (L.S.) gratefully acknowledges the support of the STA program, R. Silberberg and C. H. Tsao acknowledge the support of ONR, and A. F. Barghouty acknowledges the support of the 1992 NAVY-ASEE Faculty Summer Research Program at N.R.L.

[1] L. Sihver and T. Kanai, National Institute of Radiological Sciences Report No. NIRS-M-87, HIMAC-002, 1992.

[2] Kox *et al.*, Phys. Rev. C **35**, 1678 (1987).

[3] R. Silberberg and C. H. Tsao, Astrophys. J. Suppl. **25**, 315 (1973); **25**, 335 (1973).

[4] R. Silberberg and C. H. Tsao, in *Proceedings of the 15th International Cosmic Ray Conference, Plovdiv, 1977,* edited by B. Betev (Bulgarian Academy of Science, Plovdiv, Sofia, 1977).

[5] R. Silberberg and C. H. Tsao, in Proceedings of the 21st International Cosmic Ray Conference, Adelaide, 1990 (unpublished), Vol. 3, p. 424.

[6] R. Silberberg and C. H. Tsao, Phys. Rep. **191**, 351 (1990).

[7] J. R. Cummings, T. L. Garrard, M. H. Israel, J. Klarmann, E. C. Stone, C. J. Waddington, and W. R. Binns, Phys. Rev. C **42**, 2508 (1990); J. R. Cummings, W. R. Binns, T. L. Garrard, M. H. Israel, J. Klarmann, E. C. Stone, and C. J. Waddington, *ibid.* **35**, 2530, (1990).

[8] H. L. Bradt and Peters, Phys. Rev. **77**, 54 (1950).

[9] M. R. Shavers, S. B. Curtis, J. Miller, and W. Schimmerling, Radiat. Res. **124**, 117 (1990).

[10] I. Tanihata, Hyperfine Interact. **21**, 251 (1985).

[11] J. W. Wilson, L. W. Townsend, and F. F. Badavi, Nucl. Instrum. Methods B **18**, 225 (1987).

[12] S. Barshay, C. B. Dover, and J. P. Vary, Phys. Rev. C **11**, 360 (1975).

[13] S. Barshay, C. B. Dover, and J. P. Vary, Phys. Lett. **51B**, 5 (1974).

[14] H. H. Heckman, D. E. Greiner, P. J. Lindstrom, and H. Shwe, Phys. Rev. C **17**, 1735 (1978).

[15] L. W. Townsend and J. W. Wilson, Radiat. Res. **106**, 283 (1986).

[16] Sümmerer and D. J. Morrissey, in Proceedings of the First International Conference on Radioactive Nuclear Beams, Berkeley, California, 1989 (unpublished).

[17] W. Bauhoff, At. Data Nucl. Data Tables **35**, 447 (1986).

[18] I. Schall, D. Schardt, G. Kraft, and A. Fukumura, GSI Scientific Report No. GSI 92-1, ISSN 0174-0814, 1991, p. 306.

[19] G. Rudstam, Ph.D. thesis, University of Uppsala, 1956.

[20] G. Rudstam, Z. Naturforsch. A **21**, 1027 (1966).

[21] G. Rudstam, Nucl. Phys. **A126**, 401 (1969).

[22] I. Dostrovsky, P. Rabinowitz, and R. Bivins, Phys. Rev. **111**, 1659 (1958).

[23] R. Silberberg and C. H. Tsao, Astrophys. J. Suppl. **25**, 873 (1985).

[24] P. J. Lindstrom, G. E. Greiner, H. H. Heckman, B. Cork, and F. S. Bieser, Phys. Rev. Lett. **35**, 152 (1975).

[25] J. B. Cumming, R. W. Stoenner, and P. E. Haustein, Phys. Rev. Lett. **14**, 1554 (1976).

[26] N. T. Porile, G. D. Cole, and C. R. Rudy, Phys. Rev. C **19**, 2288 (1979).

[27] D. L. Olson, B. B. Berman, D. E. Greiner, H. H. Heckman, P. J. Lindstrom, and H. J. Crawford, Phys. Rev. C **28**, 1602 (1983).

[28] C. H. Tsao, R. Silberberg, A. F. Barghouty, L. Sihver, and T. Kanai, submitted to Phys. Rev. C.

[29] J. M. Kidd, P. J. Lindstrom, H. J. Crawford, and G. Woods, Phys. Rev. C **37**, 2613 (1988).

[30] W. R. Webber, J. C. Kish, and D. A. Schrier, Phys. Rev. C **41**, 547 (1990).

[31] J. W. Wilson, L. W. Townsend, and H. B. Bidasaria, Health Phys. **46**, 1101 (1984).

[32] P. J. Lindstrom, G. E. Greiner, and H. H. Heckman, Bull. Am. Phys. Soc. **17**, 488 (1972).

[33] G. D. Westfall, L. W. Wilson, P. J. Lindstrom, H. J. Crawford, D. E. Greiner, and H. H. Heckman, Phys. Rev. C **19**, 1309 (1979).

[34] I. Tanihata *et al.*, Phys. Lett. **160B**, 380 (1985).

[35] I. Tanihata, H. Hamagaki, O. Hashimoto, Y. Shida, N. Yoshikawa, K. Sugimotao, O. Yamakawa, T. Kobayshi, and N. Takahashi, Phys. Rev. Lett. **55**, 2676 (1985).